RSC Advances

PAPER

View Article Online
View Journal | View Issue

Cite this: *RSC Adv.*, 2014, **4**, 47297

A novel quinone/reduced graphene oxide composite as a solid-phase redox mediator for chemical and biological Acid Yellow 36 reduction†

Hong Lu, Haikun Zhang, Jing Wang,* Jiti Zhou and Yang Zhou

Received 18th August 2014
Accepted 11th September 2014

DOI: 10.1039/c4ra08817d

www.rsc.org/advances

A novel quinone-modified graphene material was developed to enhance the catalytic performance of graphene for the transformation of environmental pollutants. Graphene oxide (GO) was first reduced with diethylenetriamine and the obtained NH_2-RGO was further covalently modified with anthraquinone-2-sulfonic acid (AQS). The prepared AQS-modified RGO (AQS-RGO) was characterized by XPS, IR and SEM, respectively. The catalytic performance of AQS-RGO was investigated during azo dye Acid Yellow 36 (AY 36) decolorization. It was shown that pH and temperature had significant effects on AY 36 chemical decolorization by Na_2S. At the pH of 6.0, AQS-RGO exhibited better catalytic performance compared with NH_2-RGO due to the lower activation energy of the AQS-RGO amended system. AY 36 bio-decolorization could be enhanced in a dose-dependent manner with AQS-RGO. In the presence of 25 mg L^{-1} AQS-RGO, the AY 36 bio-decolorization rate was 6.7-fold higher than that mediated by NH_2-RGO, indicating that AQS-RGO is a better electron-transfer mediator. Based on the above results, the electron transfer pathways of AQS-RGO-mediated AY 36 decolorization were proposed. These findings indicate that the application of AQS-RGO is a feasible method to enhance the treatment of azo dye-containing wastewater.

1. Introduction

Graphene is composed of atom-thick sheets of sp^2-bonded carbon atoms densely packed in a honeycomb crystal lattice, and this unique chemical structure gives graphene many outstanding electrical and mechanical properties.[1–5] Thus, graphene is widely used in sensors, nanoelectronics, biomedicine, capacitors and photocatalysts.[6–11] Graphene also shows excellent performance in the adsorption of many environmental pollutants, such as heavy metals, anionic and cationic dyes, antibiotics and pesticides.[12–15] Recently, graphene, which is generally prepared by the reduction of graphene oxide (GO),[1] has been proven to be capable of mediating the reduction of environmental contaminations. Ma *et al.*[14] reported that ethylenediamine-reduced GO (ED-RGO) effectively reduced toxic Cr(VI) to less toxic Cr(III) with the assistance of π electrons on the carbocyclic six-membered ring of ED-RGO. Further studies found that the reduced GO (RGO) by Na_2S could mediate the reduction of nitrobenzene.[16] During this process, RGO as an electron conductor accelerated electron transfer from Na_2S to nitrobenzene. These findings indicate that RGO could enhance the removal of environmental pollutants.

Different from RGO, soluble quinone compounds (SQCs) can be used as redox mediators to accelerate the reductive transformation of refractory environmental pollutants by mediating the electron transfer.[17–20] The reductive transformation process includes two steps: the reduction of SQCs and then the oxidation of reduced SQCs by refractory environmental pollutants (*e.g.* azo dyes). The redox activities of SQCs are much higher than that of RGO. Thus, it is possible that SQCs-modified graphene will greatly improve the catalytic ability of graphene to remove various environmental pollutants. Additionally, SQCs immobilized on graphene can effectively avoid the discharge of SQCs in practical application. Castelaín *et al.*[21] ever use an adsorption method to prepare a hybrid material composed of graphene and polymer endowed with anthraquinone pendant groups. However, the catalytic performance of this material is not investigated.

Azo dye, which has a toxic impact on aquatic life, are wildly used in dye-stuff manufacture industries and the azodye-containing wastewater is a threat to the environment.[17] Thus, a model azo dye Acid Yellow 36 (AY 36) was selected as a substrate. In the present study, anthraquinone-2-sulfonic sodium (AQS) as a model quinone compound was grafted on RGO using a chemical method. To our knowledge, covalent surface modification of RGO using SQCs is first reported. The catalytic effects of AQS-modified RGO (AQS-RGO) on chemical

Key Laboratory of Industrial Ecology and Environmental Engineering (China Ministry of Education), School of Environmental Science and Technology, Dalian University of Technology, Dalian 116024, China. E-mail: jwangcn@sina.com; Fax: +86 411 84706252; Tel: +86 411 84706250

† Electronic supplementary information (ESI) available. See DOI: 10.1039/c4ra08817d

and biological decolorization of AY 36 were investigated in detail, respectively.

2. Materials and methods

2.1. Materials and chemical

Graphite powder was purchased from Sinopharm chemical reagent Co., Ltd (Shanghai, China). AQS was purchased from Sigma Co., Ltd. AY 36 used in this study was purchased from Tianjin Tianshun Chemical Co., Ltd (Tianjin, China). All other reagents used were of the highest analytical grade. Anaerobic sludge was taken from the secondary settling tank of a municipal wastewater treatment plant in Dalian, where the conventional activated sludge process was used. The AS was maintained at 4 °C under anaerobic conditions before use.

2.2. Preparation of AQS-RGO and its characterization

AQS-RGO was obtained by the following two-step procedure: firstly, 0.1 g graphene oxide (GO) was dispersed into 100 mL deionized water (pH = 10 adjusted by adding ammonia). Then 3 mL diethylenetriamine as a reducing agent was added into the mixed solution after it was heated to 98 °C using water bath. The diethylenetriamine reduced GO (NH_2-RGO) was separated and washed with deionized water after 6 h of reaction; secondly, NH_2-RGO reacted with 5.0 mM anthraquinone-2-sulfonyl chloride (ASC) for 1 h at 30 °C in 100 mL dichloromethane–ethyl alcohol mixture (50 : 50 v/v), then AQS-RGO was separated and washed with dichloromethane, ethanol and distilled water successively. The obtained NH_2-RGO and AQS-RGO were dried for the following decolorization experiments. ASC was synthesized using AQS as described by Feng *et al.*[22]

GO was prepared from graphite power using a modified method of Hummers by the following steps: graphite powder (1 g) was mixed with 46 mL H_2SO_4 and 10 mL HNO_3 in an ice bath (4 °C). $KMnO_4$ (6 g) was slowly added into the mixture in 20 min and stirred for 2 h. The solution was heated at 35 °C for 12 h, and diluted with 46 mL ultrapure water. The solution was then heated at 98 °C for 2 h, and diluted by adding 200 mL ultrapure water, followed by slowly adding 20 mL H_2O_2 (30% v/v). Finally, the black graphite suspension was converted into a bright yellow graphite oxide solution. Graphite oxide precipitates were isolated by centrifugation (8000 × *g*, 30 min) and washed with HCl (1% v/v) and ultrapure water. The GO solution was eventually sonicated for 3 h and dried at 40 °C for 24 h.

X-ray photoelectron spectroscopy (XPS) and a fourier transform infrared spectrometer (FTIR, EQUINOX55, German) were used to investigate the chemical compositional changes on the surfaces of GO, NH_2-RGO and AQS-RGO. The morphologies of these materials were also analyzed using a scanning electron microscopy (SEM, KYKY-AMRAY-1000B, USA).

2.3. The catalytic performance of AQS-RGO

The catalytic performance of AQS-RGO on AY 36 decolorization was investigated as follows: (1) abiotic incubations to achieve the chemical decolorization of AY 36 with Na_2S as an electron donor; (2) microbial incubations to perform AY 36 decolorization by anaerobic sludge using glucose as an electron donor. All experimental treatments were performed in triplicate.

2.3.1. Chemical decolorization of AY 36. Experiments were performed in 50 mL phosphate buffer solution (130 mL serum bottles) containing 25 mg L^{-1} AQS-RGO, 4 mM Na_2S and 0.2 mM AY 36. These bottles were sealed with rubber stoppers and the gas headspace was flushed for 10 min with nitrogen gas. Then the bottles were incubated at 30 °C in an anaerobic chamber. Controls without sulfide were also performed. Effects of pH (5–8) and temperature (20–55 °C) on AQS-RGO mediated AY 36 decolorization were investigated. Repeated tests of AQS-RGO were also performed.

2.3.2. Biological decolorization of AY 36. Incubations were performed in 50 mL basal medium (130 mL serum bottles) containing 2.7 g VSS (volatile suspended solids) L^{-1} anaerobic sludge, 25 mg L^{-1} AQS-RGO, 0.2 mM AY 36 and 2 g L^{-1} glucose as an electron donor. Basal medium (g L^{-1}) consisted of NH_4Cl 1.0, HCOONa 1.0, $K_2HPO_4 \cdot 3H_2O$ 8.0, $NaH_2PO_4 \cdot 2H_2O$ 2.3, NaCl 10, $MgCl_2 \cdot 2H_2O$ 0.02, $CaCl_2 \cdot 2H_2O$ 0.02 (pH = 7.2). These bottles were sealed with rubber stoppers and the gas headspace was flushed for 10 min with nitrogen gas. They were finally incubated at 30 °C in a dark shaker with 150 rpm. The control experiments without AQS-RGO/NH_2-RGO or anaerobic sludge were also performed.

2.4. Analytical methods

The concentration of azo dye AY 36 was determined spectrophotometrically at its corresponding maximum visible absorption wavelength (448 nm). The decolorization products of AY 36 from reaction systems were identified using triple quad LC-MS (Agilent 6410B) with ZORBAX Eclipse plus C18 (2.1 × 150 mm). The mobile phase was composed of methanol and water containing 0.1% acetic acid. The elution program began with 10% (v/v) methanol, then linearly increased to 90% in 8 min and the flow rate was 0.3 mL min^{-1}. MS was performed under the following conditions: electrospray ionization source (ESI), CDL temperature 250 °C, block temperature 200 °C, detector pressure 1.6 V. The decolorization efficiency was expressed as (color) removal (%) = $(C_0 - C_t)/C_0 \times 100\%$, where C_0 and C_t were the AY 36 concentrations at time zero and time t (h), respectively. A zero-order model could be applied to describe the kinetics of AY 36 chemical decolorization. The zero-order rate constant k_1 (mol L^{-1} h^{-1}) was determined.

$$C_t = -k_1 t \quad (1)$$

A pseudo-first-order model was used to describe the kinetics of AY 36 bio-decolorization. The first-order rate constant k_2 (h^{-1}) was determined.

$$\ln C_0/C_t = k_2 t \quad (2)$$

A conventional three-electrode system was employed using a platinum sheet as a counter electrode, an Ag/AgCl as a reference electrode and a glassy carbon electrode (GCE) as a working electrode. Cyclic voltammetric responses were obtained for 0.3 mM

potassium ferricyanide in 0.1 M H_2SO_4 at a scan rate of 20 mV s^{-1} when GCE, NH_2-RGO/GCE and AQS-RGO/GCE, respectively, were used as working electrodes.

3. Results and discussion

3.1. Characterization of AQS-RGO

To facilitate the preparation of AQS-RGO, GO was first reduced using diethylenetriamine. During this process, hydroxy, carboxyl and epoxy groups were partly removed, and the obtained RGO was modified with amine groups (Fig. 1). As shown in Fig. S1,† the characteristic peaks of GO appear at 3430 cm^{-1} (hydroxyl group), 1741 cm^{-1} (C═O in carboxyl group) and 1053 cm^{-1} (C–O–C in the epoxide group). In the infrared spectrum of NH_2-RGO, the intensity of the –OH stretching vibration peak at 3430 cm^{-1} decreased significantly, and the peaks at 1741 cm^{-1} and 1053 cm^{-1} disappeared. Meanwhile, the characteristic absorption peaks of –CONH bonds at 1648 cm^{-1} (mainly C═O stretching) and 1552 cm^{-1} (NH deformation coupled with C–N stretching) are observed. These results indicate that $–NH_2$ has been grafted on RGO. In the infrared spectrum of AQS-RGO, the peak at 1648 cm^{-1} (C═O) became stronger compared with that of NH_2-RGO. Moreover, the characteristic adsorption peaks of C–S at 586 cm^{-1} and S═O at 1126 cm^{-1} and 1347 cm^{-1} are also observed (Fig. S1†), suggesting that RGO has been successfully modified by AQS.

The surface chemical compositions and chemical states of GO, NH_2-RGO and AQS-RGO were also analyzed by XPS. Fig. S2† shows the increased intensity of C 1s peak and the decreased intensity of O 1s peak in the spectrum of NH_2-RGO compared with those in the spectrum of GO, indicating the reduction of GO by diethylenetriamine. Meanwhile, the appearance of N 1s peak at 397.6 eV and S 2p peak at 166.9 eV in the spectra of NH_2-RGO and AQS-RGO, respectively are observed. All these observations suggest the successful surface modification of RGO by the AQS molecules. XPS analysis shows that the immobilization efficiency is approximately 0.016 mmol AQS g^{-1} RGO.

The SEM images of GO, NH_2-RGO and AQS-RGO are shown in Fig. S3.† The surface of GO sheets is relatively smooth and their edges are stratiform (Fig. S3a and b†). After reacting with diethylenetriamine, the surface of NH_2-RGO becomes rougher than that of GO. Moreover, the edges of NH_2-RGO sheets are more irregular than those of GO sheets. The surface of AQS-RGO is porous, which is convenient for microbial adsorption. The edges of AQS-RGO sheets are even more irregular than those of NH_2-RGO sheets, probably because the presence of AQS prevents the re-stacking of the RGO sheets (Fig. S3c and d†).

3.2. AQS-RGO-mediated chemical decolorization of AY 36

During AQS-RGO-mediated decolorization of AY36, the effect of pH was first investigated using Na_2S as an electron donor. Fig. S4† shows that AY 36 decolorization efficiency increased with the increase of pH from 5.0 to 6.0 in the presence of 25 mg L^{-1} AQS-RGO. At the pH of 6.0, AQS-RGO mediated decolorization efficiency reached 93% in 3 h. When pH was over 6.5, AY 36 decolorization efficiency began to decrease. It seems that the delivery of a certain amount of protons is required for the reduction of azo bonds (–N═N–).

At the pH of 6, the catalytic effect of AQS-RGO on AY 36 decolorization was compared with those of NH_2-RGO and GO. Fig. 2a shows that only 14% decolorization occurred in 3 h in the control system and GO-supplemented system. AY 36 decolorization rates increased at various levels, when NH_2-RGO or AQS-RGO was added into reaction systems, respectively. NH_2-RGO ($k = 0.5616 \times 10^{-4}$ mol L^{-1} h^{-1}, $R^2 = 0.99$) and AQS-RGO ($k = 0.6399 \times 10^{-4}$ mol L^{-1} h^{-1}, $R^2 = 0.99$) exhibited more significantly accelerating effects on decolorization compared with GO ($k = 0.0997 \times 10^{-4}$ mol L^{-1} h^{-1}, $R^2 = 0.99$). Moreover, AQS-RGO-mediated AY 36 decolorization rate increased approximately 15% over that mediated by NH_2-RGO. Repeated tests showed that the decolorization efficiency of AQS-RGO-mediated AY 36 (0.2 mM) could remain over 95% of its original value after 5 cycles (Fig. 2b). These results demonstrated that AQS-RGO exhibits good stability and catalytic performance for AY 36 decolorization by sulfide.

For NH_2-RGO and AQS-RGO supplemented systems, the effect of temperature on AY 36 decolorization was further investigated. Fig. 3 shows that AY 36 decolorization rate reduced

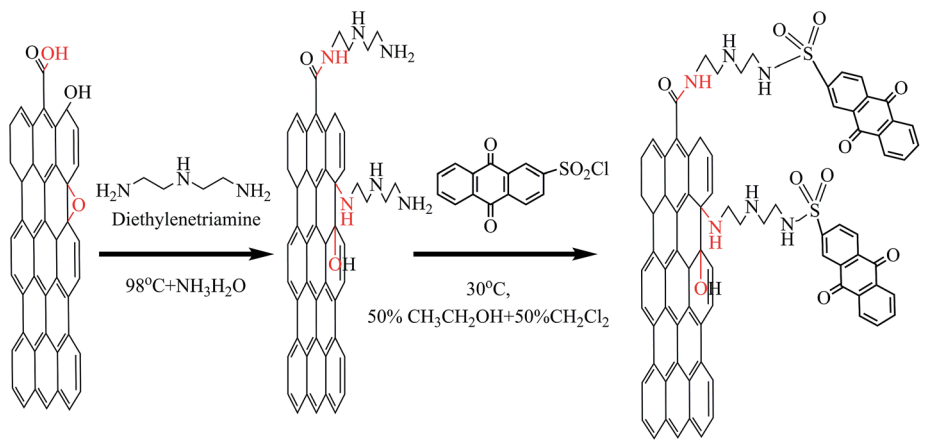

Fig. 1 Schematic illustration of the preparation of AQS-RGO.

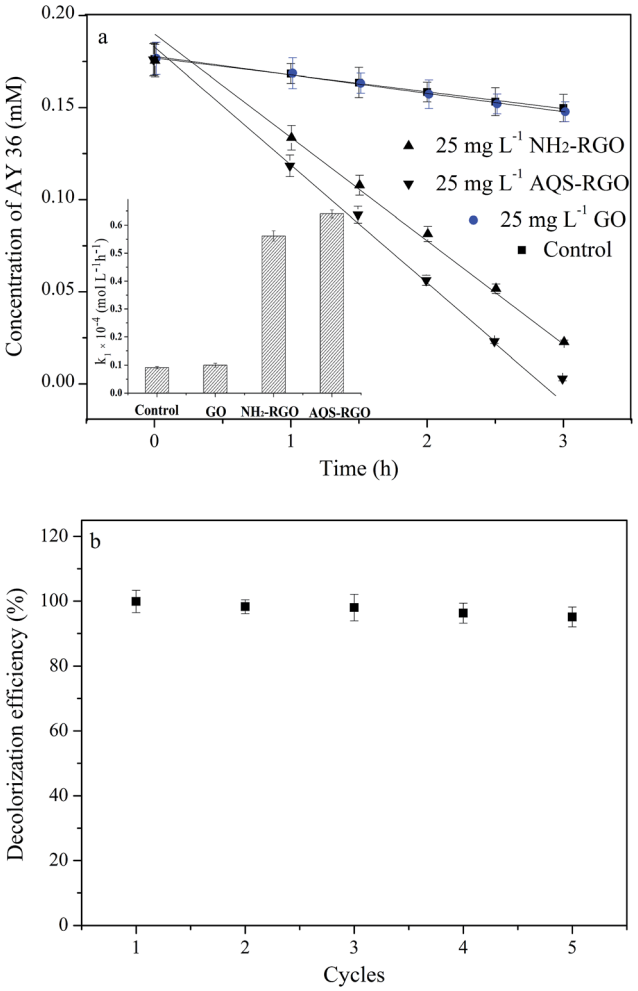

Fig. 2 (a) Effects of GO, NH_2-RGO and AQS-RGO on AY 36 decolorization in Na2S-containing aqueous solution. (b) Repeated usage experiments of AQS-RGO. Reaction conditions: 30 °C, 0.2 mM AY 36, 4 mM Na2S and 25 mg L^{-1} AQS-RGO.

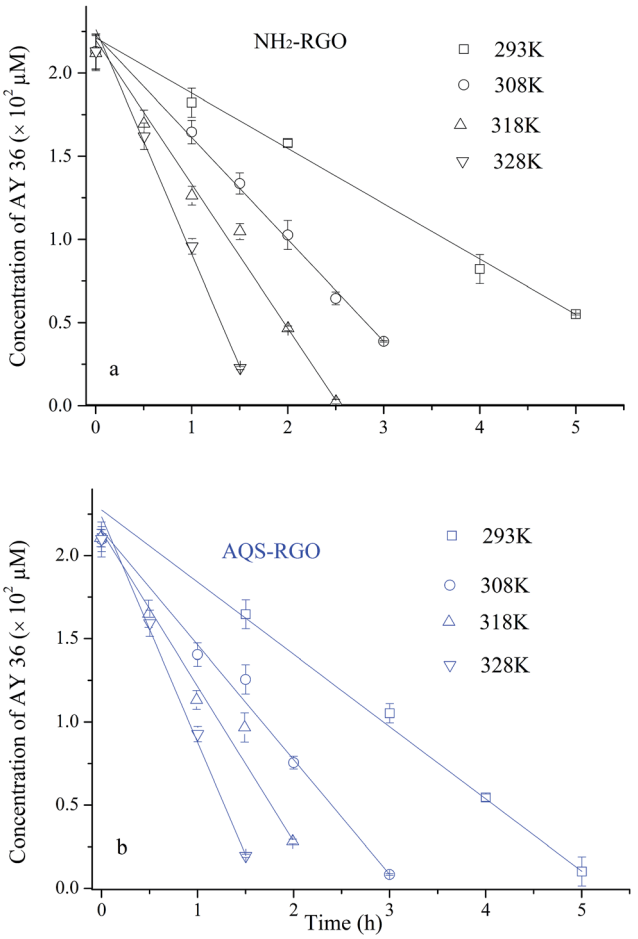

Fig. 3 Effect of temperature on the decolorization of AY 36 mediated by NH_2-RGO (a) and AQS-RGO (b) in Na_2S-containing aqueous solution. Reaction conditions: 0.2 mM AY 36, 4 mM Na_2S and 25 mg L^{-1} NH_2-RGO/AQS-RGO.

with the decrease of temperature. This decolorization process follows the zero-order kinetics in each temperature tested. The zero-order rate constant (k_1) was determined and shown in Table 1. The eqn (3) was used to calculate Arrhenius activation energy:

$$\ln k_1 = \ln A - E_a/RT \quad (3)$$

where k_1 (mol L^{-1} h^{-1}) is zero-order rate constant, A is Arrhenius factor, R (8.314 J mol^{-1} K^{-1}) is ideal gas constant, E_a (kcal mol^{-1}) is activation energy, T (K) is temperature. Table 1 shows that the calculated E_a values are 6.12 kcal mol^{-1} and 7.54 kcal mol^{-1} for AQS-RGO and NH_2-RGO supplemented systems, respectively, indicating that the presence of AQS resulted in the decrease of activation energy. Dos Santos *et al.*[23] also found that the activation energy decreased during the chemical decolorization of Reactive Red 2 due to the addition of AQS. Our results showed that the AQS-RGO mediated AY 36 decolorization has a lower potential barrier compared with NH_2-RGO. The thermodynamic parameters including $\Delta H^{\#}$ (activation enthalpy change) and $\Delta S^{\#}$ (activation entropy change) were also calculated using Eyring eqn (4).

$$\ln(k_1/T) = \ln(k_B/T) + \Delta S^{\#}/R - \Delta H^{\#}/(RT) \quad (4)$$

where k_B (J K^{-1}) is a Boltzmann constant. The values of $\Delta H^{\#}$ and $\Delta S^{\#}$ were shown in Table 1. The negative entropy values indicate that randomness on the interface of catalyst-solution decreased during the catalytic reduction process.

3.3. AQS-RGO mediated bio-decolorization of AY 36

Previous studies showed that bacterial activities (such as *E. coli*) substantially decreased with the increase of RGO or GO concentration, due to the direct contact between cells and the extremely sharp edges of GO or RGO.[24] In the present study, SEM images show that the surface of AQS-RGO sheets was rougher and their edges were more irregular compared with GO. Thus, the effect of AQS-RGO concentration on AY 36 bio-decolorization by anaerobic sludge was investigated at the temperature of 30 °C and optimal pH of 7.0. Fig. S5† shows that with the AQS-RGO concentration of 75 mg L^{-1}, the

Table 1 Kinetic and thermodynamic parameters for AY 36 decolorization mediated by NH_2-RGO and AQS-RGO

Materials	T (K)	$k_1 \times 10^{-4}$ (mol L^{-1} h^{-1})	r_0^2	E_a (kcal mol^{-1})	r_A^2	$\Delta H^{\#}$ (kcal mol^{-1})	$\Delta S^{\#}$ (J mol^{-1} K^{-1})	r_e^2
NH_2-RGO	293	0.3325	0.9942	7.5394	0.9947	6.9247	−339.4984	0.9939
	308	0.6136	0.9963					
	318	0.8657	0.9903					
	328	1.3533	0.9946					
AQS-RGO	293	0.4344	0.9949	6.1219	0.9904	5.5071	−359.7282	0.9886
	308	0.6901	0.9941					
	318	0.9313	0.9653					
	328	1.3565	0.9944					

decolorization efficiencies of AY 36 reached 99%, while AY 36 removal in the system without AQS-RGO only reached 50% in 5 h. When the concentration of additional AQS-RGO was over 100 mg L^{-1}, it was found that the accelerating effect of AQS-RGO on AY 36 decolorization declined. This result suggests that AY 36 bio-decolorization could be enhanced in dose-dependent manner of AQS-RGO. Wang *et al.*[25] reported that nitrogen removal was inhibited in the presence of 150 mg L^{-1} RGO. However, in this study, the addition of 150 mg L^{-1} AQS-RGO significantly enhanced AY 36 decolorization, indicating that AQS-RGO is of better biological compatibility than RGO. A possible explanation is that the edge of AQS-RGO becomes less sharp than that of RGO, resulting in the lower toxicity to cells.

At AQS-RGO of 25 mg L^{-1}, AQS-RGO mediated bio-decolorization of AY 36 was compared with those mediated by GO and NH_2-RGO. Fig. 4 shows that no decolorization occurred in 5 h in the control systems without anaerobic sludge, indicating that the adsorption effects of GO, NH_2-RGO and AQS-RGO could be neglected. AY 36 bio-decolorization follows pseudo-order kinetics reaction. The addition of GO ($k = 0.0364$ h^{-1}, $R^2 = 0.99$) only slightly increased AY 36 bio-decolorization ($k = 0.0327$ h^{-1}, $R^2 = 0.99$), while NH_2-RGO and AQS-RGO could significantly accelerate AY 36 decolorization. In particular, AQS-RGO-mediated decolorization of AY 36 ($k = 0.8827$ h^{-1}, $R^2 = 0.93$) was 6.7-fold higher than that mediated by NH_2-RGO ($k = 0.1310$ h^{-1}, $R^2 = 0.96$), indicating AQS-RGO is a better electron-transfer mediator. Moreover, AQS-RGO displayed more significant catalytic performance for AY 36 bio-decolorization compared with chemical decolorization, perhaps because microorganisms in anaerobic sludge are capable of reducing quinone well. It was reported that many quinone-reducing community could be enriched from anaerobic sludge.[26,27]

The decolorization products of AY 36 were further analyzed using LC-MS. N^1-phenylbenzene-1,4-diamine, one decolorization product, was detected during both chemical and biological decolorizations (Fig. S6†). After complete decolorization, AY 36 was not detected in samples (data not shown). These results meant that the azo bond of AY 36 was broken down and AY 36 was reduced to corresponding amines, which was consistent with previous reports on azo dye bio-decolorization by bacteria.[28–30]

The electrical conductivity of RGO provides an excellent opportunity to improve the bio-transformation performance of organic pollutants. Quinonyl group of SQCs has good redox

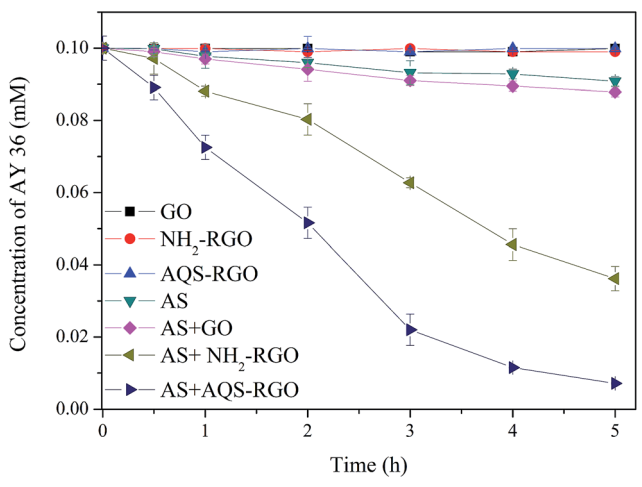

Fig. 4 Profiles of AY 36 bio-decolorization mediated by GO, NH_2-RGO and AQS-RGO, respectively. Reaction conditions: 30 °C, 0.1 mM AY 36, 2.6 g L^{-1} anaerobic sludge (AS) and 25 mg L^{-1} GO/NH_2-RGO/AQS-RGO.

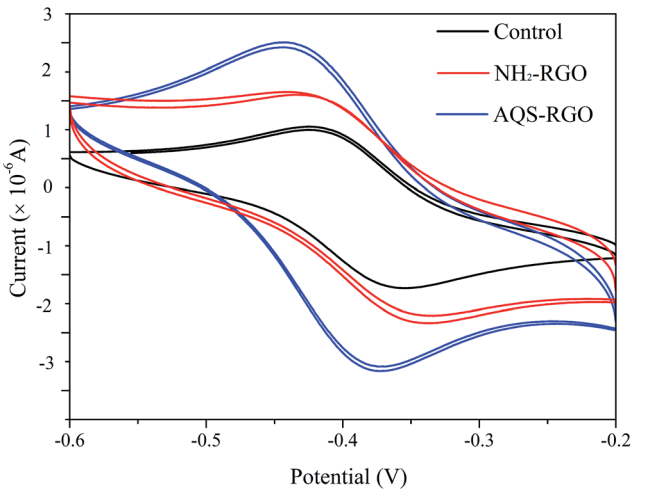

Fig. 5 Cyclic voltammetric responses obtained for 0.3 mM potassium ferricyanide in 0.1 M H_2SO_4 at a scan rate of 20 mV s^{-1} using glassy carbon electrode (GCE), NH_2-RGO/GCE and AQS-RGO/GCE, respectively.

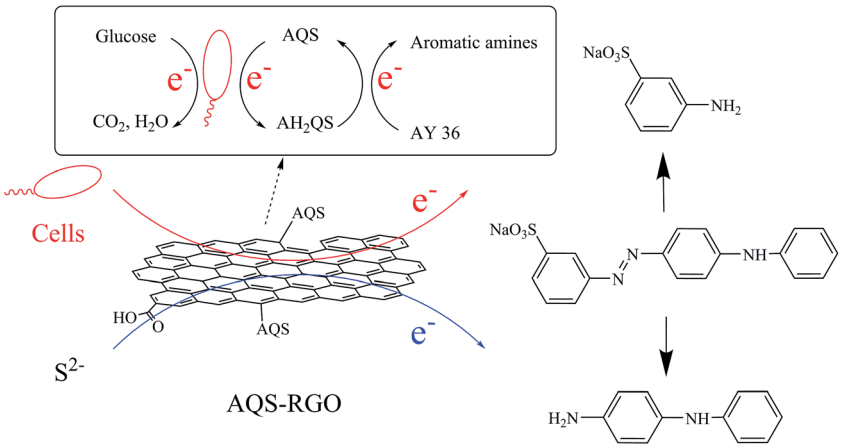

Fig. 6 Proposed electron transfer pathways for AQS-RGO-mediated AY 36 reduction.

activity. Therefore, SQCs-modified RGO is supposed to have better ability to transfer electrons. In the present study, AQS-RGO exhibited the best catalytic performance, followed by NH_2-RGO and GO. This result is also supported by the cyclic voltammetric responses of the above materials. As shown in Fig. 5, when NH_2-RGO and AQS-RGO modified GCEs were used, the redox peak currents increased remarkably and peak potentials shifted more negatively compared with unmodified GCE, suggesting that NH_2-RGO and AQS-RGO possess electrocatalytic activities, and the electrocatalytic activity of the latter is superior to that of the former.

Previous studies demonstrated that both QCs and RGO could enhance the electron transfer during the chemical/biological reduction of organic contaminants.[16,29,31] Combined with our experimental results, the electron transfer pathways of AQS-RGO-mediated AY 36 reduction were proposed (Fig. 6). During this process, AQS is first reduced by microorganisms or Na_2S and the formed hydroquinones (AH_2QS) reduce AY 36 in the purely chemical redox reaction. AQS, with the support of RGO, rapidly channeled the electrons derived from electron donors (*e.g.* Na_2S and glucose) to AY 36, resulting in the increased decolorization of AY 36.

4. Conclusions

In this paper, AQS-modified RGO was prepared using chemical method. At the pH of 6.0, AQS-RGO exhibited better catalytic performance for AY 36 chemical decolorization compared with NH_2-RGO due to the lower activation energy of AQS-RGO supplemented system. Compared with AY 36 chemical decolorization, AQS-RGO displayed more significantly accelerating effect on bio-decolorization at the AQS-RGO concentration of 25 mg L^{-1}. During the above decolorization process, AY 36 was reduced to the corresponding aromatic amines. These results indicate that AQS-RGO can efficiently accelerate azo dye reduction and has potential application in the treatment of azo dye-containing wastewater.

Acknowledgements

This subject was supported by National Natural Science foundation of China (no. 21077019).

References

1 A. K. Geim, Graphene: status and prospects, *Science*, 2009, **324**, 1530–1534.
2 C. Gómez-Navarro, R. T. Weitz, A. M. Bittner, M. Scolari, A. Mews, M. Burghard and K. Kern, Electronic transport properties of individual chemically reduced graphene oxide sheets, *Nano Lett.*, 2007, **7**, 3499–3503.
3 Z. J. Fan, W. Kai, J. Yan, T. Wei, L. J. Zhi, J. Feng, Y. M. Ren, L. P. Song and F. Wei, Facile synthesis of graphene nanosheets via Fe reduction of exfoliated graphite oxide, *ACS Nano*, 2011, **5**, 191–198.
4 M. Q. Yang, N. Zhang, M. Pagliaro and Y. J. Xu, Artificial photosynthesis over graphene-semiconductor composites. Are we getting better?, *Chem. Soc. Rev.*, 2014, DOI: 10.1039/c4cs00213j.
5 N. Zhang, M. Q. Yang, Z. R. Tang and Y. J. Xu, Toward improving the graphene-semiconductor composite photoactivity via the addition of metal ions as Generic Interfacial Mediator, *ACS Nano*, 2014, **8**, 623–633.
6 A. K. Geim and K. S. Novoselov, The rise of graphene, *Nat. Mater.*, 2007, **6**, 183–191.
7 M. J. Allen, V. C. Tung and R. B. Kaner, Honeycomb carbon: A review of graphene, *Chem. Rev.*, 2010, **110**, 132–145.
8 Y. Zhu, S. Murali, W. Cai, X. Li, J. W. Suk, J. R. Potts and R. S. Ruoff, Graphene and graphene oxide: Synthesis, properties, and applications, *Adv. Mater.*, 2010, **22**, 3906–3924.
9 N. Zhang, Y. H. Zhang and Y. J. Xu, Recent progress on graphene-based photocatalysts: current status and future perspectives, *Nanoscale*, 2012, **4**, 5792–5813.
10 M. Q. Yang and Y. J. Xu, Selective photoredox using graphene-based composite photocatalyst, *Phys. Chem. Chem. Phys.*, 2013, **15**, 19102–19118.

11 Y. H. Zhang, N. Zhang, Z. R. Tang and Y. J. Xu, Graphene transforms wide band gap ZnS to a visible light photocatalyst. The new role of graphene as a macromolecular photosensitizer, *ACS Nano*, 2012, **6**, 9777–9789.

12 V. Chandra, J. Park, Y. Chun, J. W. Lee, I. C. Hwang and K. S. Kim, Water-dispersible magnetite-reduced graphene oxide composites for arsenic removal, *ACS Nano*, 2010, **4**, 3979–3986.

13 V. Chandra and K. S. Kim, Highly selective adsorption of Hg^{2+} by a polypyrrole-reduced graphene oxide composite, *Chem. Commun.*, 2011, **47**, 3942–3944.

14 H. L. Ma, Y. Zhang, Q. H. Hu, D. Yan, Z. Z. Yu and M. Zhai, Chemical reduction and removal of Cr(VI) from acidic aqueous solution by ethylenediamine-reduced graphene oxide, *J. Mater. Chem.*, 2012, **22**, 5914–5916.

15 T. Kuila, S. Bose, A. K. Mishra, P. Khanra, N. H. Kim and J. H. Lee, Chemical functionalization of graphene and its applications, *Prog. Mater. Sci.*, 2012, **57**, 1061–1105.

16 H. Fu and D. Zhu, Graphene oxide-facilitated reduction of nitrobenzene in sulfide-containing aqueous solutions, *Environ. Sci. Technol.*, 2013, **47**, 4204–4210.

17 J. Rau, H. J. Knackmuss and A. Stolz, Effects of different quinoid redox mediators on the anaerobic reduction of azo dyes by bacteria, *Environ. Sci. Technol.*, 2002, **36**, 1497–1504.

18 E. J. O'Loughlin, Effects of electron transfer mediators on the bioreduction of lepidocrocite (γ-FeOOH) by *Shewanella putrefaciens* CN32, *Environ. Sci. Technol.*, 2008, **42**, 6876–6882.

19 F. Luan, W. D. Burgos, L. Xie and Q. Zhou, Bioreduction of nitrobenzene, natural organic matter, and hematite by *Shewanella putrefaciens* CN32, *Environ. Sci. Technol.*, 2010, **44**, 184–190.

20 B. Gu, H. Yan, P. Zhou and D. B. Watson, Natural humics impact uranium bioreduction and oxidation, *Environ. Sci. Technol.*, 2005, **39**, 5268–5275.

21 M. Castelaín, H. J. Salavagione, R. Gómez and J. L. Segura, Supramolecular assembly of graphene with functionalized poly (fluorene-*alt*-phenylene): the role of the anthraquinone pendant groups, *Chem. Commun.*, 2011, **47**, 7677–7679.

22 F. Feng, B. J. Uno, M. Goto, Z. X. Zhang and D. K. An, Anthraquinone-2-sulfonyl chloride: a new versatile derivatization reagent – synthesis mechanism and application for analysis of amines, *Talanta*, 2002, **57**, 481–490.

23 A. B. dos Santos, I. A. Bisschops, F. J. Cervantes and J. B. van Lier, Effect of different redox mediators during thermophilic azo dye reduction by anaerobic granular sludge and comparative study between mesophilic (30 °C) and thermophilic (55 °C) treatments for decolourisation of textile wastewaters, *Chemosphere*, 2004, **55**, 1149–1157.

24 O. Akhavan and E. Ghaderi, Toxicity of graphene and graphene oxide nanowalls against bacteria, *ACS Nano*, 2010, **4**, 5731–5736.

25 D. Wang, G. Wang, G. Zhang, X. Xu and F. Yang, Using graphene oxide to enhance the activity of anammox bacteria for nitrogen removal, *Bioresour. Technol.*, 2013, **131**, 527–530.

26 L. Li, J. Wang, J. Zhou, F. Yang, C. Jin, Y. Qu, A. Li and L. Zhang, Enhancement of nitroaromatic compounds anaerobic biotransformation using a novel immobilized redox mediator prepared by electropolymerization, *Bioresour. Technol.*, 2008, **99**, 6908–6916.

27 Y. Su, Y. Zhang, J. Wang, J. Zhou, X. Lu and H. Lu, Enhanced bio-decolorization of azo dyes by co-immobilized quinone-reducing consortium and anthraquinone, *Bioresour. Technol.*, 2009, **100**, 2982–2987.

28 C. I. Pearce, R. Christie, C. Boothman, H. von Canstein, J. T. Guthrie and J. R. Lloyd, Reactive azo dye reduction by *Shewanella* strain J18 143, *Biotechnol. Bioeng.*, 2006, **95**, 692–703.

29 Y. G. Hong, J. Guo, Z. C. Xu, M. Y. Xu and G. P. Sun, Humic substances act as electron acceptor and redox mediator for microbial dissimilatory azoreduction by *Shewanella decolorationis* S12, *J. Microbiol. Biotechnol.*, 2007, **17**, 428–437.

30 A. Khalid, M. Arshad and D. E. Crowley, Decolorization of azo dyes by Shewanella sp. under saline conditions, *Appl. Microbiol. Biotechnol.*, 2008, **79**, 1053–1059.

31 E. D. Brutinel and J. A. Gralnick, Shuttling happens: soluble flavin mediators of extracellular electron transfer in *Shewanella*, *Appl. Microbiol. Biotechnol.*, 2012, **93**, 41–48.